ARTICLES

Chd1 regulates open chromatin and pluripotency of embryonic stem cells

Alexandre Gaspar-Maia[1,2,3], Adi Alajem[4], Fanny Polesso[1,2], Rupa Sridharan[5], Mike J. Mason[5], Amy Heidersbach[2], João Ramalho-Santos[6], Michael T. McManus[2], Kathrin Plath[5], Eran Meshorer[4] & Miguel Ramalho-Santos[1,2]

An open chromatin largely devoid of heterochromatin is a hallmark of stem cells. It remains unknown whether an open chromatin is necessary for the differentiation potential of stem cells, and which molecules are needed to maintain open chromatin. Here we show that the chromatin remodelling factor Chd1 is required to maintain the open chromatin of pluripotent mouse embryonic stem cells. Chd1 is a euchromatin protein that associates with the promoters of active genes, and downregulation of Chd1 leads to accumulation of heterochromatin. Chd1-deficient embryonic stem cells are no longer pluripotent, because they are incapable of giving rise to primitive endoderm and have a high propensity for neural differentiation. Furthermore, Chd1 is required for efficient reprogramming of fibroblasts to the pluripotent stem cell state. Our results indicate that Chd1 is essential for open chromatin and pluripotency of embryonic stem cells, and for somatic cell reprogramming to the pluripotent state.

The genome of eukaryotic cells is organized into accessible euchromatin that is permissive for gene activation, and packaged heterochromatin that is largely silenced. Different cellular states may be defined at least in part by differential allocation of genomic regions to specific chromatin domains[1]. Several types of stem cells in organisms ranging from planarians[2] to mammals[3,4] have been reported to have an open chromatin largely devoid of heterochromatin. This phenomenon has been analysed in greater detail in pluripotent mouse embryonic stem (ES) cells. These cells have an open, 'loose' chromatin with high rates of histone protein exchange, and accumulate regions of more rigid heterochromatin after differentiation[5,6]. An open chromatin correlates with a globally permissive transcriptional state, and has been proposed to contribute to the developmental plasticity, or pluripotency, of ES cells[6]. Although there is a strong correlation between open chromatin and the undifferentiated state of stem cells, it remains unknown whether open chromatin is necessary for stem cell potential. Furthermore, little is known about the molecules that may regulate open chromatin in stem cells. Here we report the identification of the chromatin remodeller Chd1 as an essential regulator of open chromatin and pluripotency of ES cells, and of somatic cell reprogramming to pluripotency.

Chd1 regulates ES cell self-renewal

We have recently characterized the transcriptional profiles of pluripotent stem cells, including ES cells, and the cells in the mouse embryo from which they are derived (ref. 7 and G. Wei, R.-F. Yeh, M. Hebrok and M.R.-S., unpublished observations). These studies led to the identification of chromatin remodellers and transcription factors upregulated in pluripotent cells. To test the role of 41 candidate factors in the regulation of pluripotency, we carried out an RNA interference (RNAi) screen in ES cells (Supplementary Fig. 1). ES cells expressing green fluorescent protein (GFP) under the control of the *Oct4* promoter (Oct4-GiP) were infected with a short hairpin RNA (shRNA)-expressing lentiviral vector, pSicoR-mCherry[8]. Using 1–2 shRNAs per candidate target gene, we identified 18 genes that when downregulated led to defects in expansion of ES cells, and 7 that led to lower activity of the *Oct4* promoter. *Chd1* was the only gene with phenotypes in both assays that had not been previously implicated in ES cells (Supplementary Fig. 1).

Chd1 is a chromatin-remodelling enzyme that belongs to the chromodomain family of proteins and contains an ATPase SNF2-like helicase domain[9]. The two chromodomains in Chd1 are essential for recognition of histone H3 di- or tri-methylated at lysine 4 (H3K4me2/3; ref. 10), and Chd1 has been implicated in transcriptional activation in yeast[11], *Drosophila*[12] and mammalian cells[13]. Recent transcription factor location studies indicate that the *Chd1* gene is bound in mouse ES cells by Oct4 (also known as Pou5f1), Sox2, Nanog, Smad1, Zfx and E2f1, suggesting that it is a target of several regulators of pluripotency and self-renewal[14].

RNAi against *Chd1* in Oct4-GiP ES cells, using two independent shRNAs targeting different regions of the messenger RNA, led to a decrease in the expansion of ES cells and to lower Oct4–GFP levels (Fig. 1a, b and Supplementary Fig. 2a). Control cells were infected with empty pSicoR-mCherry or with pSicoR-mCherry expressing an shRNA targeting GFP (empty and GFP RNAi, respectively), and behaved like uninfected cells (Supplementary Figs 1d and 2a). Downregulation of *Chd1* mRNA after RNAi was confirmed by reverse transcription followed by quantitative PCR (qRT–PCR) (Supplementary Fig. 2b). Endogenous *Oct4* downregulation was confirmed in Chd1-deficient (*Chd1* RNAi) ES cells (Supplementary Fig. 3a). *Oct4* downregulation induced differentiation into the trophectoderm lineage[15] (marked by *Cdx2* and *Eomes*), unlike knockdown of *Chd1*, indicating that the *Chd1* RNAi phenotype is not simply one of trophectoderm differentiation due to the loss of *Oct4* (Supplementary Fig. 3).

Chd1 downregulation decreased clonogenic potential in two independent ES cell lines (Oct4-GiP and E14), but *Chd1* RNAi cells were

[1]Departments of Ob/Gyn and Pathology, Center for Reproductive Sciences and Eli and Edythe Broad Center of Regenerative Medicine and Stem Cell Research, University of California, San Francisco, 513 Parnassus Avenue, San Francisco, California 94143-0525, USA. [2]Diabetes Center, University of California, San Francisco, California 94143-0534, USA. [3]PhD Programme in Biomedicine and Experimental Biology (BEB), Center for Neuroscience and Cell Biology, University of Coimbra, 3004-517 Coimbra, Portugal. [4]Department of Genetics, Institute of Life Sciences, The Hebrew University of Jerusalem, Jerusalem 91904, Israel. [5]Department of Biological Chemistry and Eli and Edythe Broad Center of Regenerative Medicine and Stem Cell Research, University of California, Los Angeles, PO Box 951737, Los Angeles, California 90095, USA. [6]Center for Neuroscience and Cell Biology, University of Coimbra, 3004-517 Coimbra, Portugal.

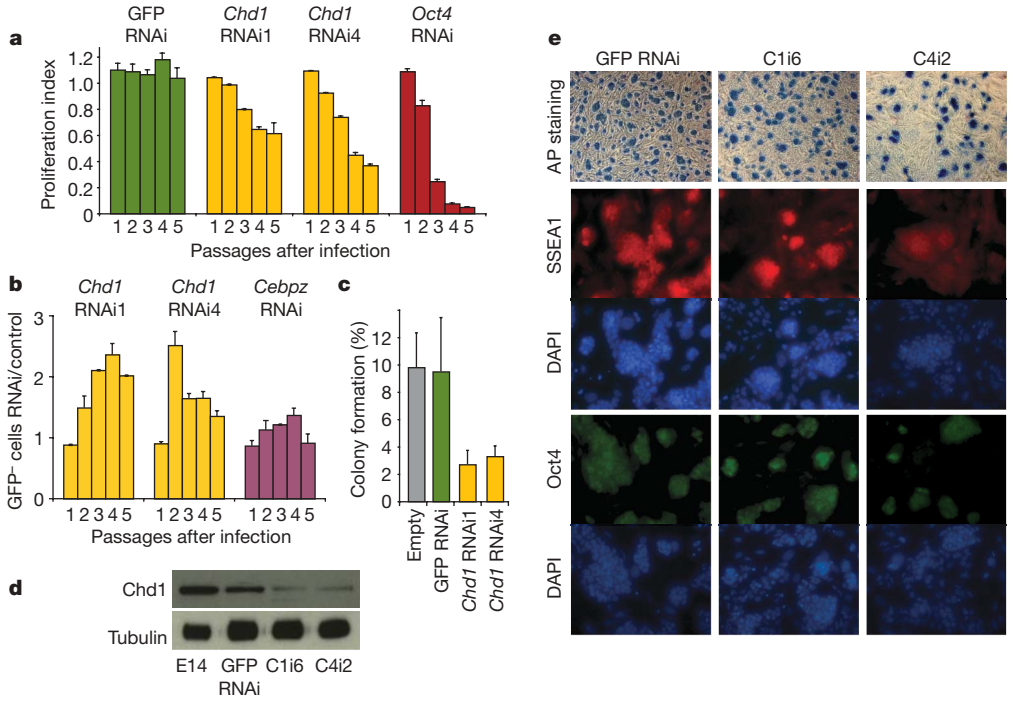

Figure 1 | *Chd1* RNAi ES cells have decreased self-renewal but maintain expression of markers of the undifferentiated state. a, A competition assay shows that downregulation of *Chd1* in Oct4-GiP ES cells using two independent shRNAs (*Chd1* RNAi1 and *Chd1* RNAi4) leads to a decreased proliferative capacity. The proliferation index represents the population of mCherry^{+} cells relative to cells infected with empty vector, at each time point. Experiments were done in triplicate and are represented as mean and s.d. ($n = 3$). **b**, Downregulation of *Chd1* leads to reduced activity of the Oct4–GFP reporter, as measured by the ratio between the percentage of GFP-negative cells in RNAi and in empty vector. *Chd1* RNAi cells have a twofold increase of GFP-negative cells relative to controls for at least one passage. Downregulation of a different gene that affects only proliferation (*Cebpz*) has little effect on Oct4–GFP expression. Data are mean and s.d. ($n = 3$). **c**, The efficiency of colony formation in *Chd1* RNAi ES cells was decreased relative to controls (empty and GFP RNAi). Data are mean and s.d. ($n = 3$), and are representative of two independent experiments. **d**, Immunoblot with whole cell extracts from parental E14 cells, GFP RNAi and two *Chd1* RNAi ES cell clones (C1i6 and C4i2) using antibodies against Chd1 or α-tubulin. **e**, *Chd1* RNAi cells still express markers of undifferentiated ES cells, such as alkaline phosphatase (AP; shown in bright field; original magnification, ×100), and SSEA1 and Oct4 (shown with immunofluorescence; original magnification, ×400). Nuclei were stained with 4,6-diamidino-2-phenylindole (DAPI).

still able to form ES-like colonies (Fig. 1c), unlike *Oct4* RNAi ES cells. ES cell clones constitutively expressing either of the two shRNAs against *Chd1* were established, and sustained *Chd1* downregulation was verified by qRT–PCR (see below Supplementary Fig. 5) and western blot (Fig. 1d). Control lines were established using empty and GFP RNAi viruses. As described later, the two shRNAs targeting *Chd1* led to identical phenotypes in marker gene expression, transcriptional profile, differentiation potential and chromatin state, relative to controls. Results were validated in the two independent ES cell lines Oct4-GiP and E14. The data are from analyses in standard E14 ES cells not expressing GFP. *Chd1* RNAi ES cells, even though they have a self-renewal defect, form compact colonies and express markers of ES cells, such as SSEA1, alkaline phosphatase and Oct4 (Fig. 1e), indicating that they maintain at least some aspects of the undifferentiated state.

Chd1 is required for ES cell pluripotency

To gain insight into the state of *Chd1* RNAi ES cells, we determined their global gene expression profiles using Affymetrix mouse Gene 1.0 ST microarrays (Supplementary Fig. 4). We anticipated that we would find a pattern of downregulated genes in *Chd1* RNAi cells, because Chd1 is known to be associated with active transcription[13]. As expected, both *Chd1* and *Oct4* were found to be downregulated in *Chd1* RNAi ES cells. Surprisingly, however, very few other genes were significantly downregulated (only 25 genes were downregulated more than twofold and none more than threefold at 90% confidence, Supplementary Fig. 4b and Supplementary Data 1). These data indicate that, at least with the low levels of *Chd1* still present in *Chd1* RNAi ES cells, there is a global maintenance of the ES cell transcriptome. On the other hand, a larger group of genes was upregulated in *Chd1* RNAi ES cells (Supplementary Fig. 4b and Supplementary Data 1). A Gene Ontology (GO) analysis of the list of upregulated transcripts showed a significant enrichment for genes involved in neurogenesis (Supplementary Fig. 4c), such as nestin and *Blbp* (also known as *Fabp7*), which was confirmed by qRT–PCR (Supplementary Fig. 5d).

The maintenance of the ES cell transcriptome and the unexpected expression of neural markers were further analysed by immunofluorescence for nestin, Blbp and Oct4. Oct4 was detected in *Chd1* RNAi colonies, but cells between the colonies stained strongly for Blbp (Fig. 2a) and nestin (Supplementary Fig. 4e). No staining for nestin or Blbp was detected in control ES cells. These results were confirmed with fluorescence-activated cell sorting (FACS) using the ES cell marker SSEA1 (Supplementary Fig. 5). In summary, *Chd1* RNAi ES cells can be propagated with many of the hallmarks of the undifferentiated state, but have a high propensity for neuronal differentiation.

We next tested the differentiation potential of *Chd1* RNAi ES cells *in vitro* by the formation of embryoid bodies. *Chd1* RNAi embryoid bodies did not form the typical outer layer of primitive endoderm, as marked by immunofluorescence of embryoid body sections with Afp and Gata4 (Fig. 2b). Similarly, yolk sac endoderm cysts were reduced or not observed in *Chd1* RNAi embryoid bodies (Supplementary Fig. 6a), which showed downregulation of primitive endoderm markers (*Gata4*, *Afp*, *Hnf4a* and *Lamb*) by qRT–PCR (Supplementary Fig. 6b). The loss of primitive endoderm in *Chd1* RNAi embryoid bodies was comparable to that in embryoid bodies lacking an essential regulator of primitive endoderm, *Gata6* (ref. 16) (Fig. 2b). Beating foci, indicative of cardiac mesoderm differentiation, were not detected in *Chd1* RNAi embryoid bodies, whereas they could be readily

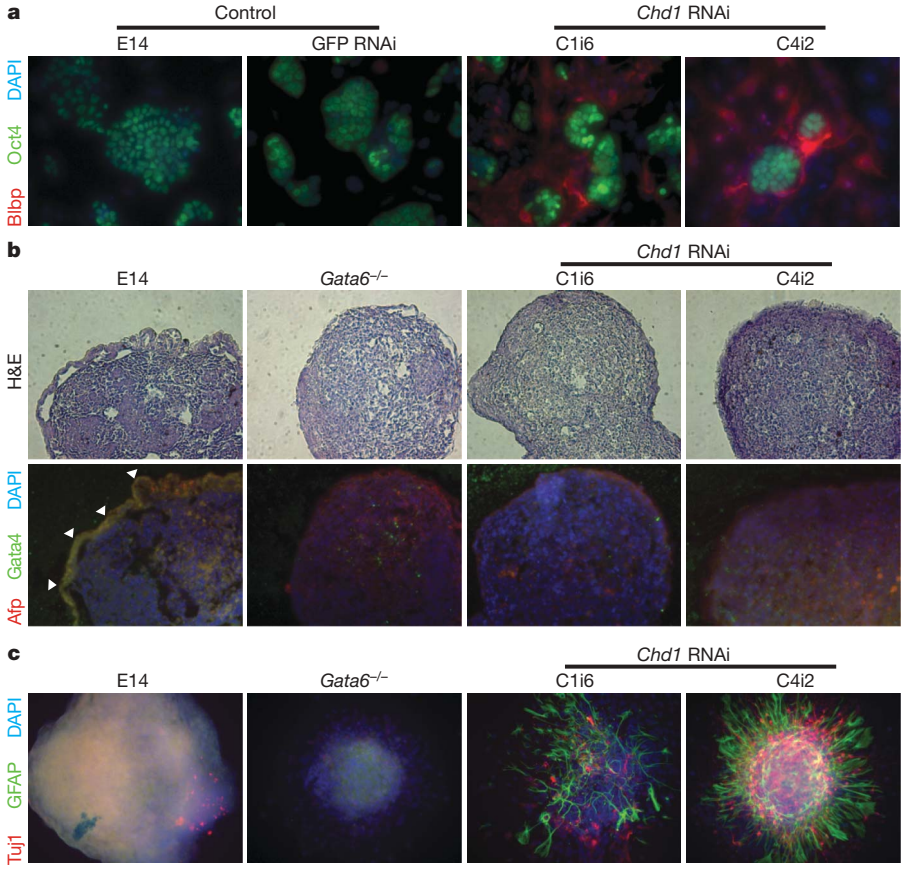

Figure 2 | Chd1 is required for ES cell pluripotency. a, Immunofluorescence analysis of *Chd1* RNAi cells shows expression of Blbp (red), but in a population not expressing the ES cell marker Oct4 (green). Original magnification, ×400. **b**, Paraffin sections of 6 day embryoid bodies were stained for Afp (red) and Gata4 (green), or haematoxylin and eosin (H&E). The loss of the primitive endoderm layer (highlighted in control GFP RNAi by white arrowheads) in *Chd1* RNAi embryoid bodies is similar to that observed in embryoid bodies mutant for *Gata6*. Original magnification, ×100. **c**, A significant increase in neural differentiation is observed, as detected by staining embryoid bodies (plated on matrigel) for astrocytes (GFAP in green) and neurons (Tuj1 in red), in 12 day *Chd1* RNAi embryoid bodies, relative to controls. Nuclei were stained with DAPI. Original magnification, ×200.

quantified in control embryoid bodies (Supplementary Fig. 6c). However, beating foci were also not observed in *Gata6*$^{-/-}$ embryoid bodies, indicating that the loss of cardiac mesoderm differentiation in *Chd1* RNAi embryoid bodies may be secondary to the loss of primitive endoderm. Immunostaining of *Chd1* RNAi embryoid bodies plated on matrigel showed a marked increase of neurons (stained with Tuj1) and astrocytes (stained with Gfap) relative to controls (Fig. 2c). This increase in neural differentiation is not secondary to the loss of primitive endoderm, because *Gata6*$^{-/-}$ embryoid bodies did not show such phenotype (Fig. 2c). Furthermore, *Chd1* RNAi ES cells gave rise to teratomas with abundant neuronal differentiation when compared to wild-type ES cells (Supplementary Fig. 7). These results indicate that downregulation of Chd1 leads to loss of primitive endoderm, with consequential loss of cardiac mesoderm differentiation, and abnormally high levels of neural differentiation that derives from a propensity already detected in the undifferentiated state.

Chd1 is a euchromatin protein in ES cells

We then sought to understand the potential changes in the chromatin state of *Chd1* RNAi ES cells that may underlie their differentiation defects. Previous studies[11–13] indicated that Chd1 associates with euchromatin by binding to H3K4me3, although genome-wide location studies had not been performed. We carried out chromatin immunoprecipitation (ChIP)-chip for Chd1 in wild-type ES cells, and compared the genome-wide location of Chd1 to that of H3K4me3, RNA polymerase II (Pol II) and H3K27me3. These data showed that Chd1 binding strongly correlates with that of Pol II and H3K4me3 (Fig. 3 and Supplementary Fig. 8). Bivalent domains, simultaneously enriched for both the activating H3K4me3 mark and repressive H3K27me3 mark[17], are largely devoid of Chd1 (Fig. 3a and Supplementary Fig. 8). Interestingly, GO analysis indicated that the strongest Chd1 and Pol II targets are enriched for roles in DNA binding, translation and chromatin assembly genes, and that this enrichment is not strictly correlated with expression levels (Fig. 3b and Supplementary Data 2). Chd1 binding also correlates with H3K4me3 enrichment after differentiation: during embryoid body formation, the levels of both H3K4me3 and Chd1 are decreased at the *Oct4* promoter and increased at the endodermal regulator *Gata4* promoter (Supplementary Fig. 9). These data indicate that Chd1 associates globally with euchromatin in ES cells, and may preferentially target genes with roles in chromatin organization and transcription.

Chd1 is required for maintenance of open chromatin

To investigate the effects of Chd1 downregulation on ES cell chromatin, we performed immunofluorescence for histone marks of euchromatin and heterochromatin. Surprisingly, foci of heterochromatin marks such as H3K9me3 and HP1γ (also known as Cbx3), which normally appear as dispersed foci in ES cells[5], were markedly increased in *Chd1* RNAi ES cells (Fig. 4a and Supplementary Fig. 10). No obvious differences were observed in staining for H3K4me3 or H3K27me3 between *Chd1* RNAi ES cells and controls (data not shown). As described earlier, *Chd1* RNAi ES cells are prone to spontaneous neural

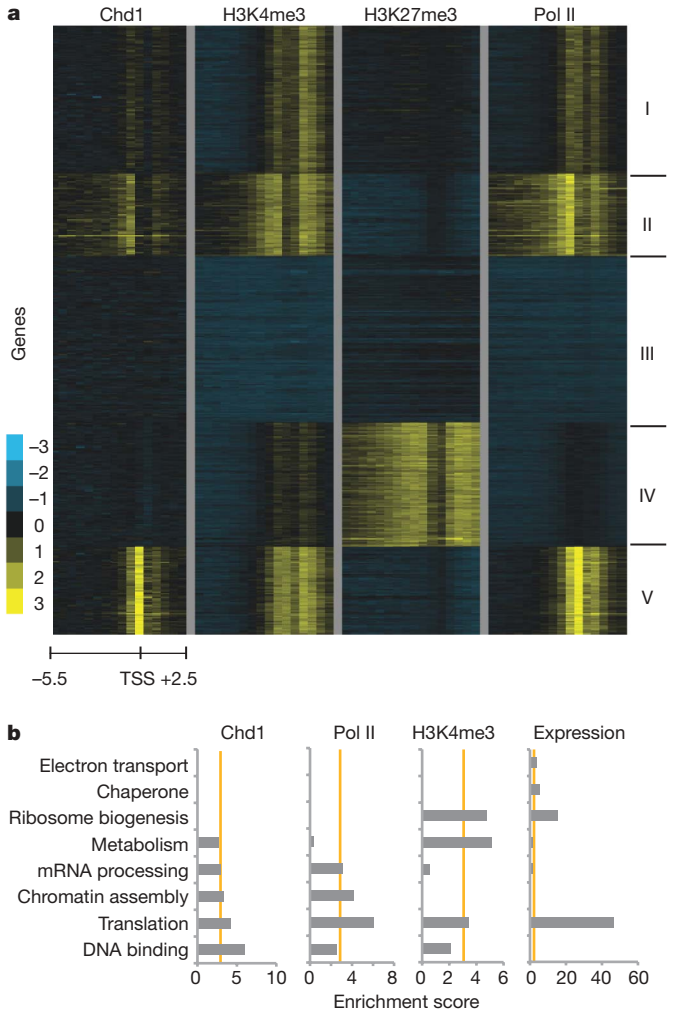

Figure 3 | Chd1 associates with euchromatic promoter regions in ES cells. **a**, K-means clustering of Chd1, H3K4me3, H3K27me3 and RNA Pol II binding in ES cells. Chd1 binding correlates with binding of H3K4me3 and RNA Pol II but is excluded from bivalent domains (cluster IV) in ES cells. Each row represents the binding pattern along the −5.5 kilobase (kb) to +2.5 kb promoter region relative to the transcription start site (TSS). **b**, Functional categorization of Chd1 targets. Gene Ontology (GO) terms associated with the 200 genes most strongly bound by Chd1 or RNA Pol II, or enriched for H3K4me3, as well as the top 200 genes in expression level in ES cells. Categories above an enrichment score of three (*x* axis) are considered significantly enriched. Sixty-nine genes overlap between the Chd1 and the RNA Pol II top 200 gene lists, versus 27 for Chd1 and expression, and 13 for Chd1 and H3K4me3.

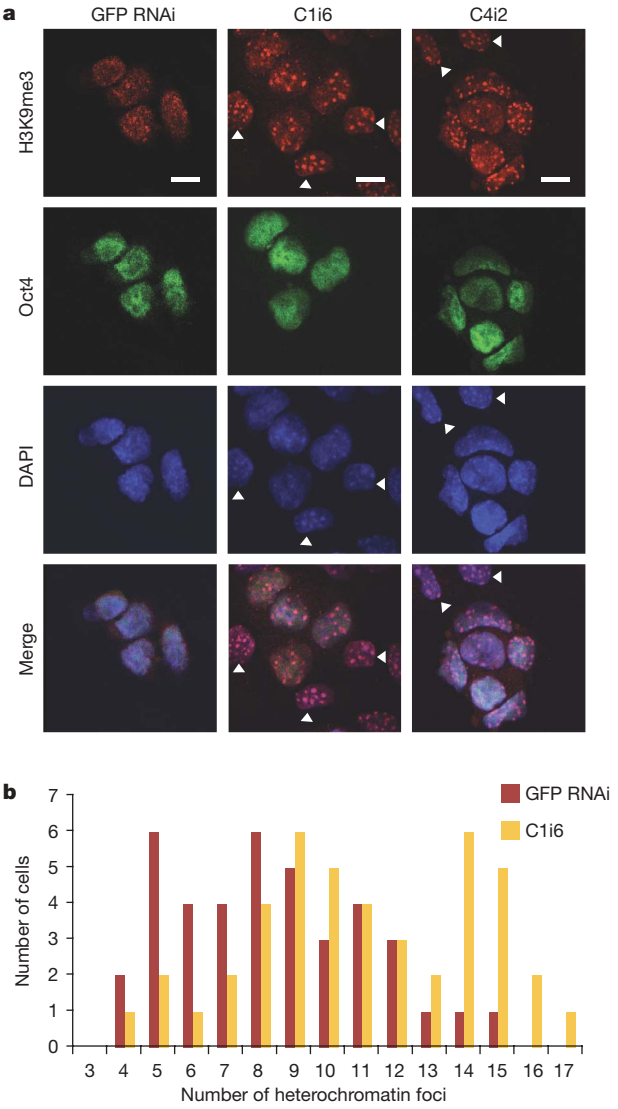

Figure 4 | Chd1 is required to maintain open chromatin in ES cells. **a**, Analysis of H3K9me3 staining by immunofluorescence. Co-staining for H3K9me3 and Oct4 distinguishes between ES-like cells (Oct4-positive) and differentiating cells (Oct4-negative, white arrowheads). Oct4-positive *Chd1* RNAi ES-like cells have increased heterochromatin foci. Scale bar, 10 μm **b**, Quantification of the increase of heterochromatin foci per nucleus in *Chd1* RNAi ES-like cells, as seen by H3K9me3 staining in Oct4-positive cells; $P < 0.0005$.

differentiation, and it has been shown that ES cell-derived neural precursors accumulate heterochromatin[5]. It was therefore important to evaluate whether the accumulation of heterochromatin is a consequence of commitment to the neural lineage, or whether it is present in ES-like cells before differentiation. Co-staining with H3K9me3 and Oct4 revealed that Oct4-positive ES-like cells, located in the centre of compact colonies that stain for other markers of the undifferentiated state (Fig. 1e), have accumulated high levels of heterochromatin in *Chd1* RNAi cells (Fig. 4a, quantified in 4b). Moreover, we analysed the global chromatin dynamics of *Chd1* RNAi cells by fluorescence recovery after photobleaching (FRAP) using a GFP-tagged histone H1. H1 is a linker protein involved in condensing nucleosomes that has been shown to rapidly exchange in the hyperdynamic chromatin of undifferentiated ES cells[5]. H1 showed a significant decrease in recovery in heterochromatin of *Chd1* RNAi ES cells, indicating that the rapid exchange of H1 is compromised (Supplementary Fig. 11). These results indicate that, despite a global maintenance of the transcriptome, morphology, and marker gene expression of ES cells, *Chd1* RNAi ES-like cells are not fully undifferentiated: their chromatin is condensed.

Heterochromatin formation is induced by methylation of H3K9 by the enzymes ESET (also known as Setdb1), Suv39H1/2, G9a (Ehmt2) or Glp (Ehmt1)[18], and reversed by the action of H3K9 demethylases such as Jmjd1a (Kdm3a) and Jmjd2c (Kdm4c). Jmjd1a and Jmjd2c have been shown to regulate genes expressed in ES cells and to repress differentiation[19]. All of these H3K9 methyltransferases and demethylases are expressed in *Chd1* RNAi ES cells at similar levels to control ES cells (Supplementary Data 1). Therefore, the accumulation of heterochromatin in *Chd1* RNAi ES cells is not likely to be due to the differential expression of known H3K9 methyltransferases or demethylases. These results indicate that the capacity to induce heterochromatin formation exists in undifferentiated ES cells, despite the presence of H3K9 demethylases, and that heterochromatinization is countered, directly or indirectly, by Chd1. Our data suggest that ES cells exist in a dynamic state of opposing epigenetic influences of euchromatin and heterochromatin, and that the

euchromatin protein Chd1 is required to maintain the heterochromatin-poor pluripotent stem cell state.

Chd1 is required for efficient induction of pluripotency

Given the role of Chd1 in maintaining pluripotency of ES cells, we hypothesized that it may also be involved in the re-acquisition of pluripotency during somatic cell reprogramming. We analysed the effect of *Chd1* downregulation (Fig. 5a, b) in the reprogramming of Oct4–GFP mouse embryonic fibroblasts (MEFs) to induced pluripotent stem (iPS) cells[20–24]. Downregulation of *Chd1*, using two independent shRNAs in three separate experiments, led to a significant reduction in the number of iPS cell colonies, scored both by morphology and GFP expression. This was not due to a delay in colony formation, as colony counts at later time points showed the same relative reduction in reprogramming efficiency after *Chd1* RNAi treatment (data not shown). The iPS cell colonies that did form in *Chd1* RNAi wells either had not been infected by the RNAi virus or had silenced it, as assessed both by *Chd1* qRT–PCR and mCherry fluorescence (Supplementary Figs 12 and 13). Downregulation of *Chd1* could potentially affect proliferation of MEFs, which would confound the calculation of reprogramming efficiency. However, no significant changes in MEF growth rates were found between control and *Chd1* RNAi (Fig. 5c). Moreover, *Chd1* RNAi does not alter the expression level of the exogenous reprogramming factors (data not shown). In summary, our data show that downregulation of Chd1 does not affect the expansion of fibroblasts but inhibits their reprogramming by induction of pluripotency.

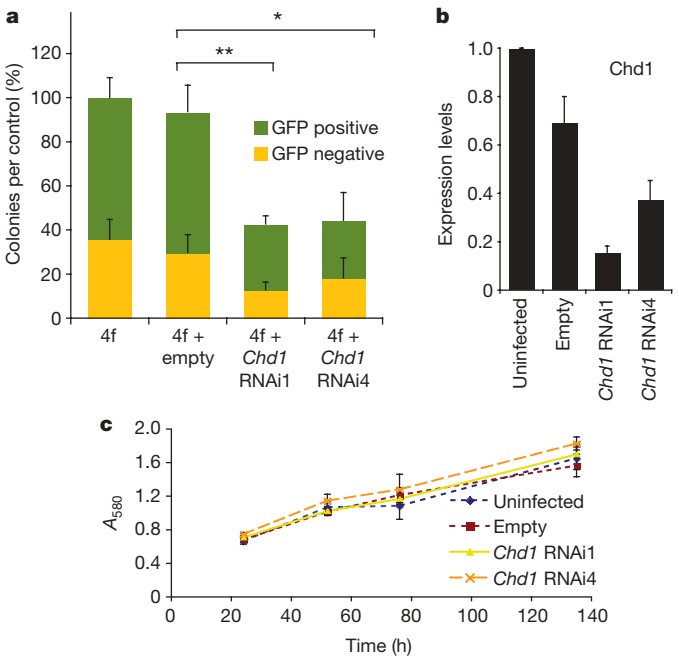

Figure 5 | Chd1 is required for efficient induction of pluripotency. a, The percentage of reprogrammed colonies was scored both by morphology and GFP expression, and normalized to the total number of colonies obtained in the control (four factors only, '4f'). The values are represented as mean and s.d. of the averages of three independent experiments, each one done in duplicate or triplicate. The total number of colonies in control wells (4f or 4f + empty) in the three separate experiments varied between 200 and 500 per 6-well. The efficiency of induction of pluripotency is significantly reduced after *Chd1* RNAi treatment. Unpaired *t*-test was performed using the total number of colonies obtained, comparing the control (empty) with RNAi against *Chd1* (*Chd1* RNAi1 and *Chd1* RNAi4). $*P < 0.0001$, $**P < 0.00001$. **b**, *Chd1* downregulation after RNAi was confirmed by qRT–PCR. The values are represented as mean of absolute expression and s.d. ($n = 3$). **c**, Mean growth rate of MEFs measured by the MTT assay and s.d. ($n = 6$). No differences in MEF growth rate were observed after *Chd1* RNAi treatment.

Discussion

We show here that Chd1 is required for open chromatin and pluripotency of ES cells. ES cells have been reported to be 'poised' for differentiation by the presence of bivalent domains (marked by H3K4me3 and H3K27me3) in developmental regulatory genes[17]. We speculate that the opposing influences of euchromatin and heterochromatin (marked by H3K9me3) may be a further mechanism for maintaining ES cells in a state poised for differentiation. Chd1 is also highly expressed in human ES cells relative to differentiated cells (Supplementary Fig. 14)[25], suggesting that its role in pluripotent stem cells may be conserved. Interestingly, it is possible that other stem cells maintain their differentiation potential using a similar mechanism, because *Chd1* has also been identified as a gene upregulated in adult haematopoietic and neural stem/progenitor cells[26]. Furthermore, our data show that Chd1 is required for efficient generation of iPS cells. Fibroblasts have much higher levels of heterochromatin than pluripotent stem cells[5] (and data not shown), and therefore a global opening of the chromatin is expected to be a component of reprogramming. Our data suggest that Chd1 may contribute to opening the chromatin and enabling transcription-factor-mediated reprogramming to occur, although the precise mechanisms remain to be determined.

It is unclear how Chd1, a protein associated with euchromatin, acts to counter heterochromatinization. Recent genetic studies in yeast indicate that euchromatin-associated factors prevent spreading of heterochromatin to euchromatic regions[27,28]. Further studies will be required to determine whether Chd1 has a similar role in ES cells. An intriguing possibility is that Chd1 may mediate incorporation of the histone variant H3.3, which is generally associated with active genes and is less prone to H3K9 methylation[29]. In support of this model, Chd1 has recently been shown to be required in the *Drosophila* oocyte for incorporation of H3.3 into sperm chromatin, a step necessary for development[30]. In addition, a genome-wide analysis of the chromatin state of *Chd1* RNAi ES cells may provide insight into the differential sensitivity of endoderm and neural lineages to chromatin condensation.

METHODS SUMMARY

The RNAi screen was performed in Oct4-GiP ES cells using the lentiviral vector pSicoR-mCherry. A proliferation index was derived from a competition assay between infected and non-infected cells analysed by flow cytometry over five passages. Oct4-GiP and E14 *Chd1* RNAi and control ES cell clones were expanded from $mCherry^+$ cells isolated by FACS, and validated by qRT–PCR for *Chd1* downregulation. ES clones and embryoid bodies were grown in standard culture conditions. For expression microarray experiments, RNA from E14 *Chd1* RNAi and control clones was amplified and hybridized to Affymetrix Mouse Gene 1.0 ST arrays. Normalized data was analysed in dChip. Gene Ontology analyses were done with MAPPFinder or DAVID. For ChIP-chip, immunoprecipitated DNA was amplified and hybridized to Agilent G4490 promoter arrays. Data were extracted as previously described[31] and visualized using Cluster 3.0 and Treeview. ChIP, qRT–PCR and western blotting were performed using standard protocols. Immunofluorescence was performed on matrigel-coated chamber slides, with ES cells or embryoid bodies plated 2 days before fixation, or on paraffin-sectioned embryoid bodies. Teratomas were generated by subcutaneous injection of ES cells into SCID mice. FRAP analysis[5] and induction of pluripotency[24] were performed as described previously. Cell proliferation was measured using the MTT assay.

Full Methods and any associated references are available in the online version of the paper at www.nature.com/nature.

Received 7 April; accepted 18 June 2009.
Published online 8 July 2009.

1. Mikkelsen, T. *et al.* Dissecting direct reprogramming through integrative genomic analysis. *Nature* **454**, 49–55 (2008).
2. Reddien, P. W. & Sanchez-Alvarado, A. Fundamentals of planarian regeneration. *Annu. Rev. Cell Dev. Biol.* **20**, 725–757 (2004).
3. Terstappen, L. W. *et al.* Sequential generations of hematopoietic colonies derived from single nonlineage-committed $CD34^+CD38^-$ progenitor cells. *Blood* **77**, 1218–1227 (1991).
4. Spangrude, G. J., Heimfeld, S. & Weissman, I. L. Purification and characterization of mouse hematopoietic stem cells. *Science* **241**, 58–62 (1988).

5. Meshorer, E. *et al.* Hyperdynamic plasticity of chromatin proteins in pluripotent embryonic stem cells. *Dev. Cell* **10,** 105–116 (2006).
6. Efroni, S. *et al.* Global transcription in pluripotent embryonic stem cells. *Cell Stem Cell* **2,** 437–447 (2008).
7. Grskovic, M. *et al.* Systematic identification of *cis*-regulatory sequences active in mouse and human embryonic stem cells. *PLoS Genet.* **3,** e145 (2007).
8. Ventura, A. *et al.* Cre-lox-regulated conditional RNA interference from transgenes. *Proc. Natl Acad. Sci. USA* **101,** 10380–10385 (2004).
9. Woodage, T. *et al.* Characterization of the CHD family of proteins. *Proc. Natl Acad. Sci. USA* **94,** 11472–11477 (1997).
10. Sims, R. J. *et al.* Human but not yeast CHD1 binds directly and selectively to histone H3 methylated at lysine 4 via its tandem chromodomains. *J. Biol. Chem.* **280,** 41789–41792 (2005).
11. Simic, R. *et al.* Chromatin remodeling protein Chd1 interacts with transcription elongation factors and localizes to transcribed genes. *EMBO J.* **22,** 1846–1856 (2003).
12. Stokes, D. G., Tartof, K. D. & Perry, R. P. CHD1 is concentrated in interbands and puffed regions of *Drosophila* polytene chromosomes. *Proc. Natl Acad. Sci. USA* **93,** 7137–7142 (1996).
13. Sims, R. J. *et al.* Recognition of trimethylated histone H3 lysine 4 facilitates the recruitment of transcription postinitiation factors and pre-mRNA splicing. *Mol. Cell* **28,** 665–676 (2007).
14. Chen, X. *et al.* Integration of external signaling pathways with the core transcriptional network in embryonic stem cells. *Cell* **133,** 1106–1117 (2008).
15. Niwa, H., Miyazaki, J. & Smith, A. G. Quantitative expression of Oct-3/4 defines differentiation, dedifferentiation or self-renewal of ES cells. *Nature Genet.* **24,** 372–376 (2000).
16. Morrisey, E. E. *et al.* GATA6 regulates HNF4 and is required for differentiation of visceral endoderm in the mouse embryo. *Genes Dev.* **12,** 3579–3590 (1998).
17. Bernstein, B. E. *et al.* A bivalent chromatin structure marks key developmental genes in embryonic stem cells. *Cell* **125,** 315–326 (2006).
18. Lachner, M. & Jenuwein, T. The many faces of histone lysine methylation. *Curr. Opin. Cell Biol.* **14,** 286–298 (2002).
19. Loh, Y.-H. *et al.* Jmjd1a and Jmjd2c histone H3 Lys 9 demethylases regulate self-renewal in embryonic stem cells. *Genes Dev.* **21,** 2545–2557 (2007).
20. Takahashi, K. & Yamanaka, S. Induction of pluripotent stem cells from mouse embryonic and adult fibroblast cultures by defined factors. *Cell* **126,** 663–676 (2006).
21. Okita, K., Ichisaka, T. & Yamanaka, S. Generation of germline-competent induced pluripotent stem cells. *Nature* **448,** 313–317 (2007).
22. Maherali, N. *et al.* Directly reprogrammed fibroblasts show global epigenetic remodeling and widespread tissue contribution. *Cell Stem Cell* **1,** 55–70 (2007).
23. Wernig, M. *et al. In vitro* reprogramming of fibroblasts into a pluripotent ES-cell-like state. *Nature* **448,** 318–324 (2007).
24. Blelloch, R., Venere, M., Yen, J. & Ramalho-Santos, M. Generation of induced pluripotent stem cells in the absence of drug selection. *Cell Stem Cell* **1,** 245–247 (2007).
25. Skottman, H. *et al.* Gene expression signatures of seven individual human embryonic stem cell lines. *Stem Cells* **23,** 1343–1456 (2005).
26. Ramalho-Santos, M. *et al.* ''Stemness'': transcriptional profiling of embryonic and adult stem cells. *Science* **298,** 597–600 (2002).
27. Kimura, A., Umehara, T. & Horikoshi, M. Chromosomal gradient of histone acetylation established by Sas2p and Sir2p functions as a shield against gene silencing. *Nature Genet.* **32,** 370–377 (2002).
28. Venkatasubrahmanyam, S. *et al.* Genome-wide, as opposed to local, antisilencing is mediated redundantly by the euchromatic factors Set1 and H2A.Z. *Proc. Natl Acad. Sci. USA* **104,** 16609–16614 (2007).
29. McKittrick, E., Gafken, P. R., Ahmad, K. & Henikoff, S. Histone H3.3 is enriched in covalent modifications associated with active chromatin. *Proc. Natl Acad. Sci. USA* **6,** 1525–1530 (2004).
30. Konev, A. Y. *et al.* CHD1 motor protein is required for deposition of histone variant H3.3 into chromatin *in vivo*. *Science* **317,** 1087–1090 (2007).
31. Sridharan, R. *et al.* Role of the murine reprogramming factors in the induction of pluripotency. *Cell* **136,** 364–377 (2009).

Supplementary Information is linked to the online version of the paper at www.nature.com/nature.

Acknowledgements The authors wish to thank A. Smith for Oct4-GiP ES cells, M. S. Parmacek for *Gata6*$^{-/-}$ ES cells, R. P. Perry and D. G. Stokes for the Chd1 antibody, M. Bigos and V. Stepps at the Flow Cytometry Core Facility and L. Ta and C. Barker at the Genomics Core Facility of the Gladstone Institutes for expert assistance, C. Chiu for technical assistance, members of the Santos laboratory, in particular M. Grskovic for advice, and A. Kriegstein, D. Melton, A. Alvarez-Buylla, D. Stainier, R. Blelloch, B. Panning, J. Reiter and M. Grskovic for discussions and critical reading of the manuscript. A.G.-M. was the recipient of a predoctoral fellowship from the Foundation for Science and Technology (POCI2010/FSE), Portugal. R.S. was the recipient of a CIRM postdoctoral training grant. This work was supported by grants from the Sandler Family to M.T.M., CIRM Young Investigator Award and NIH Director's New Innovator Award to K.P., Israel Science Foundation (ISF 215/07), European Union (IRG-206872) and Alon Fellowship to E.M., and NIH Director's New Innovator Award, California Institute for Regenerative Medicine and Juvenile Diabetes Research Foundation to M.R.-S.

Author Contributions A.G.-M., J.R.-S., M.T.M., K.P., E.M. and M.R.-S. planned the project; A.G.-M., A.A., F.P., R.S., M.J.M. and A.H. performed the experiments; A.G.-M., A.A., F.P., R.S., M.J.M., K.P., E.M. and M.R.-S. analysed the data; and A.G.-M., K.P., E.M. and M.R.-S. wrote the manuscript.

Author Information Expression and ChIP-chip microarray data are deposited in the Gene Expression Omnibus (GEO) under accession number GSE16462. Reprints and permissions information is available at www.nature.com/reprints. Correspondence and requests for materials should be addressed to M.R.-S. (mrsantos@diabetes.ucsf.edu).

METHODS

ES cell culture and differentiation. Mouse E14 and Oct4-GiP ES cells[32] were plated on 0.1% gelatin-coated plates or on a feeder layer of irradiated MEFs, and maintained in DMEM (Invitrogen) supplemented with 15% knockout serum replacement (Invitrogen), 1 mM L-glutamine, 0.1 mM nonessential amino acids, 100 μg ml^{-1} penicillin, 100 μg ml^{-1} streptomycin, 1 mM sodium pyruvate, 0.1 mM 2-mercaptoethanol and recombinant LIF. Mouse *Gata6*$^{-/-}$ ES cells[16] were grown in identical conditions except that fetal bovine serum was used instead of knockout serum replacement. Embryoid bodies were formed by plating ES cells in non-attachment conditions (suspension culture) with ES cell medium with fetal bovine serum and in the absence of LIF, for 16 days. Contractile foci were counted under an inverted microscope using triplicates of 10-cm dishes per ES cell clone.

RNAi and competition assay. The genes tested in the RNAi screen were the following: *Ap2gamma* (also known as *Tcfap2c*), *Brca1*, *Cebpz*, *Chd1*, *Ddx18*, *Dmrt1*, *Dppa2*, *Dppa3* (*Stella*), *Dppa4*, *Eed*, *Foxd3*, *Hells*, *Mybl2*, *c-Myc*, *Mycbp*, *Nmyc1* (*Mycn*), *Nanog*, *Nfya*, *Nfyb*, *Nr0b1*, *Nr5a2*, *Oct4*, *Pramel4*, *Pramel5*, *Rex1* (*Zfp42*), *Rex2*, *Rbm35a* (*Esrp1*), *Sall4*, *Six4*, *Sox2*, *Suz12*, *Tcfcp2l1*, *Terf1*, *Tex292* (*Cirh1a*), *Utf1*, *Zic3*, A030007L17Rik (*Ggc2*), and Affymetrix MG_U74Av2 probe sets 160906_i_at, 135189_f_at, 97154_f_at and 98524_f_at. shRNA sequences were selected according to published criteria[33]: GFP RNAi, ACAGCCACAACGTCTATAT; *Oct4* RNAi, GAACCTGGCTAAGCTTCCA; *Chd1* RNAi1, ACATTATGATGGAGCTAAA; *Chd1* RNAi4, GTGCTACT ACAACCATTTA. All other sequences are in Supplementary Table 1. Oligonucleotides coding for the shRNAs were designed and cloned into the lentiviral vector pSicoR-mCherry as described[7]. Lentiviruses were produced as described[8]. For transduction, 10^6 ES cells were incubated with virus in 1 ml of ES cell medium (multiplicity of infection 5–10). After 1 h rotating at 37 °C, 2.5–3×10^5 cells were plated per gelatinized well of a 12-well plate. A competition assay[34] was performed by analysing cells that were passaged every two or three days. Flow cytometry was performed on a LSRII and analysed using the Flojo software. Proliferation index was measured, for every passage, by dividing the percentage of mCherry$^+$ (shRNA) with the percentage of mCherry$^+$ (empty virus). Loss of Oct4–GFP activity was measured by dividing the percentage of GFP$^-$ cells (shRNA) with the percentage of GFP$^-$ (empty virus). The calculation of the loss of Oct4/GFP expression was done with total GFP$^-$ cells rather than just GFP$^-$/mCherry$^+$ to account for potential silencing of the mCherry construct after differentiation or non-cell autonomous effects. Proliferation index data are averages of triplicates ($n = 3$) and standard error bars. mCherry$^+$ ES cells were isolated using a FACSDiVa (BD Biosciences) cell sorter.

Colony formation assay and clonal derivation. E14 and Oct4-GiP ES cells were infected with lentiviruses containing shRNAs or empty virus alone, as described above. mCherry$^+$ cells were sorted on day 5 after infection using a FACSDiVa (BD Biosciences) cell sorter. Five thousand cells were plated per 10-cm dish in triplicates. After 10 days in culture, individual clones were picked per each condition (empty virus, GFP RNAi, *Chd1* RNAi1 or RNAi4) and propagated in standard ES cell growth conditions. Plates were stained for alkaline phosphatase using a Vector kit and colonies were counted. Results are averages of triplicates and standard error bars.

Expression microarrays. Uninfected parental E14 ES cells, one clone infected with empty pSicoR-mCherry, one GFP RNAi clone and four *Chd1* RNAi clones, three from *Chd1* RNAi1 (C1i5, C1i6 and C1i9) and one from *Chd1* RNAi4 (C4i2) were grown on gelatin in ES cell culture medium. Total RNA was isolated using the RNeasy kit (Qiagen) with in-column DNase digestion. Three-hundred nanograms of total RNA per sample were amplified and hybridized to Affymetrix Mouse Gene 1.0 ST arrays according to the manufacturer's instructions at the Genomics Core Facility of the Gladstone Institutes. These arrays assay for the expression of about 35,500 transcripts. Data were normalized using robust multi-array normalization. Hierarchical clustering and calculations of differential gene expression were done using dChip (http://www.dchip.org)[35]. The full normalized data are in Supplementary Data 1. The lower bound of the 90% confidence interval of the fold change (LCB) was used as a conservative estimate of the fold change. Five-hundred-and-thirty-one transcripts with LCB > 2 in *Chd1* RNAi relative to controls were analysed in MAPPFinder[36] for enrichment of gene ontology terms. Terms with *P* values adjusted for multiple testing ≤ 0.01 were considered enriched.

Immunohistochemistry. ES cells or embryoid bodies were plated on chamber glass slides pre-coated with matrigel. ES cells were plated on a layer of irradiated MEFs. After 2 days, cells were fixed with 4% paraformaldehyde, permeabilized with PBT (PBS plus 0.1% Triton X-100) and blocked with 2% BSA plus 1% goat or donkey serum in PBT. Slides were immunostained with primary antibody in blocking solution. Alternatively, embryoid bodies in suspension (at day 6) were fixed, paraffin-embedded, sectioned (50 μm), and stained for haematoxylin and eosin or immunostained.

Primary antibodies used: SSEA1 (MC-480, Developmental Studies Hybridoma Bank (DSHB), 1:200), Oct4 (sc5279, Santa Cruz, 1:100; sc9081; Santa Cruz; 1:50), nestin (MAB353, Chemicon, 1:200), BLBP (ab32423, Abcam, 1:200), Afp (sc8977, Santa Cruz. 1:200), Gata4 (sc1237, Santa Cruz, 1:50), Tuj1 (MMS-435P, Covance, 1:250), GFAP (Z0334, Dako, 1:500), H3K4me3 (ab8580, Abcam, 1:200), H3K9me3 (07-449, Upstate, 1:100; ab8898, Abcam, 1:100), H3K27me3 (07-449, Upstate, 1:100), HP1gamma (MAB3450, Chemicon, 1:500). Secondary antibodies: Alexa Fluor 488/594 conjugated secondary antibodies (anti-mouse, anti-rabbit, or anti-goat, 1:500, Molecular Probes). Nuclei were counterstained with DAPI. The MC-480 antibody developed by D. Solter was obtained from the DSHB developed under the auspices of the NICHD and maintained by University of Iowa.

qRT–PCR. RNA was isolated according to the RNeasy kit (Qiagen), and reverse-transcribed using the iScript first strand cDNAsynthesis kit (BioRad). The cDNA reaction was diluted 1:5 in TE buffer and used in Sybr Green real-time PCR reactions (BioRad). Housekeeping genes used were ubiquitin-b and ribosomal protein L7. PCR primer sequences are available on request. Reactions were run in replicates on a MyiQ qPCR machine (BioRad) according to the manufacturer's instructions. Cycle threshold values were imported into the REST software[37] for fold-change calculations, using the housekeeping genes as controls. Values are presented in $\log_2$ scale or in absolute expression levels compared with parental E14 RNA unless otherwise indicated.

SSEA1 cell sorting. ES cells (GFP RNAi control and *Chd1* RNAi clones) were collected by trypsinization, washed in ice-cold PBS, first resuspended in staining medium (HBSS, Ca/Mg-free, no phenol red, 2% FBS) with primary mouse antibody anti-SSEA1 (MC-480, DSHB, 1:50) for 30 min on ice, and then in secondary anti-mouse IgM-PE (406507, BioLegends, 1:100) for 30 min on ice. Propidium iodide (P3566; Invitrogen) was added and live SSEA1$^+$ and SSEA1$^-$ cells were isolated using a FACSDiVa (BD Biosciences) cell sorter.

Western blotting. Whole cell extracts were prepared and measured using the Bradford assay (BioRad) for protein content. From whole ES cell extracts 30 μg of protein were resolved on SDS–PAGE gel (10%) using a rabbit antibody against Chd1 (1:2,000, from R. Perry[12]) and a goat anti-rabbit HRP (1:10,000). The loading control used was α-tubulin, detected with a mouse antibody (1:1,000, Sigma T9026). From embryoid body extracts (at day 12), 10 μg of protein were resolved on a 10% SDS–PAGE gel using an antibody against Tuj1 (1:1,000) and anti-goat HRP (1:10,000). Detection was performed using the ECL kit according to manufacturer's instructions (Amersham).

FRAP analysis. Transfection of H1–GFP into ES cells and FRAP analysis were performed as described[5].

Generation of teratomas. Teratomas were produced by injecting 3×10^6 cells subcutaneously in the flanks of SCID mice. Tumour tissue samples developed in 12 weeks and were fixed overnight in 4% paraformaldehyde before paraffin embedding. Sections were stained with haematoxylin and eosin with a standard protocol.

ChIP. ChIP was performed essentially as described by Upstate Biotechnology, with some minor changes described below: chromatin was cross-linked by incubating cells on plates with PBS containing 20 mM dimethylpimelimidate (DMP; Sigma) and 0.25% dimethylsulphoxide (DMSO) for 1 h at room temperature. Cells were re-fixed with 2% paraformaldehyde for another hour at room temperature, scraped and centrifuged at 1,350*g* for 5 min. Pellets were resuspended in SDS lysis buffer and sonicated to obtain fragments of ~200–1,000 base pairs (bp) as verified on a gel. Reactions were centrifuged at 13,000*g* for 10 min and the supernatants were used. Antibodies used (3 μg each): Chd1 (PAB-10569, Orbigen), H3K4me3 (ab8580, Abcam) IgG (ab46540, Abcam). DNA was purified by phenol–chloroform extraction, followed by ethanol precipitation. DNA concentration was determined using a Nanodrop spectrophotometer (NanoDrop Technologies) and 5–10 ng were used in Sybr Green real-time PCR reactions (see earlier) ran in duplicates or triplicates. Primer sequences are available on request. Fold enrichment over input was calculated using the $2^{\Delta Ct}$ method corrected with IgG C_t values. The HoxA3 primer set was used as a control gene because it corresponds to a region known to lack H3K4me3 (ref. 17).

ChIP-chip. ChIP and hybridization onto Agilent promoter microarrays was performed as described[22]. In brief 500 μg of crosslinked ES chromatin was immunoprecipitated with 10 μg of Chd1 antibody (Allele Biotech PAB-10568) or hypophosphorylated RNA polymerase II (8WG16). The eluate was reverse crosslinked, RNase- and proteinase-K-treated and purified. Equal amounts of input and immunoprecipitated samples were amplified using the WGA2 kit (Sigma), labelled with the Bioprime kit (Invitrogen) and hybridized onto Agilent mouse promoter arrays (G4490) according to manufacturer's instructions. Data were extracted as previously described[31]. Data were visualized using the Cluster 3.0 and Treeview programs. Bound genes were determined using the Young laboratory algorithm[38]. H3K4me3 and H3K27me3 data, as well as the algorithm to generate the 500-bp window presentation were previously published[22]. In K-means clustering, each row

represents the binding pattern along the −5.5 to +2.5 kb promoter region relative to the TSS, reiterated four times to present the data for each immunoprecipitation. The 8 kb promoter region is divided into sixteen 500 bp fragments that display the average log ratio of probe signal intensity with blue, yellow and grey representing lower-than-average, higher-than-average and missing values for enrichment due to lack of probes in those regions, respectively. The odds ratio for binary correlation of Chd1 binding strength was calculated as the ratio of the probability of a gene being bound by Chd1 divided by the probability of it being bound by H3K4me3 (or RNA Pol II or H3K27me3) to the probability of a gene being bound by Chd1 divided by the probability of the gene being unbound by H3K4me3 (or RNA Pol II or H3K27me3).

Reprogramming. Reprogramming was performed as previously described[24], with minor changes: Oct4–GFP MEFs were reprogrammed using lentiviral infection (day 0) of four transcription factors (*Oct4*, *Sox2*, *nMyc* and *Klf4*). RNAi lentiviral vectors (empty, *Chd1* RNAi1, *Chd1* RNAi4) were used to infect MEFs 4 days before the addition of the four factors. At day 1, MEFs were also plated for a MTT assay to quantify growth rates and for RNA collection for qRT–PCR for *Chd1*. An optimization of the protocol was also used and described in Supplementary Fig. 12 (as reported previously[39]). iPS colonies were scored (13 to 16 days after addition of the four factors) by GFP fluorescence, using a scale according to the number of cells in a colony that were GFP positive, as described in Supplementary Fig. 12b (GFP-positive refers to all the colonies with any GFP-positive cells), or by their morphology under bright field (GFP-negative).

MTT assay. The growth rate of MEFs was measured using an indirect method. Yellow MTT is reduced by mitochondrial enzymes into a purple formazan and the absorbance measured as a result of the number of viable cells. For the MTT assay, MEFs were plated at 5,000 cells per well in a 96-well plate and analysed 24, 52, 76 and 135 h after plating. At the indicated time points, ES cell medium (without LIF) was replaced with 100 ml 1 mg ml^{-1} 3-(4,5-dimethylthiazol-2-yl)-2.5-diphenyltetrazolium bromide (MTT) (Molecular Probes) in DMEM. After incubation at 37 °C for 3 h, the MTT solution was removed. One-hundred millilitres of DMSO was added to dissolve precipitate for 10 min at 37 °C and 5 min at room temperature. Absorbance was recorded at 540 nm using a Spectramax M2 microplate reader (Molecular Devices).

32. Ying, Q. L., Nichols, J., Evans, E. P. & Smith, A. G. Changing potency by spontaneous fusion. *Nature* **416,** 545–548 (2002).
33. Reynolds, A. *et al.* Rational siRNA design for RNA interference. *Nature Biotechnol.* **22,** 326–330 (2004).
34. Ivanova, N. *et al.* Dissecting self-renewal in stem cells with RNA interference. *Nature* **442,** 533–538 (2006).
35. Li, C. & Wong, W. H. Model-based analysis of oligonucleotide arrays: expression index computation and outlier detection. *Proc. Natl Acad. Sci. USA* **98,** 31–36 (2001).
36. Doniger, S. W. *et al.* MAPPFinder: using Gene Ontology and GenMAPP to create a global gene-expression profile from microarray data. *Genome Biol.* **4,** R7 (2003).
37. Pfaffl, M. W., Horgan, G. W. & Dempfle, L. Relative expression software tool (REST) for group-wise comparison and statistical analysis of relative expression results in real-time PCR. *Nucleic Acids Res.* **30,** e36 (2002).
38. Boyer, L. A. *et al.* Polycomb complexes repress developmental regulators in murine embryonic stem cells. *Nature* **441,** 349–353 (2006).
39. Wernig, M. *et al.* A drug-inducible transgenic system for direct reprogramming of multiple somatic cell types. *Nature Biotechnol.* **26,** 916–924 (2008).